

SYNTHESIS, CHARACTERIZATION, AND ANTIBACTERIAL STUDY OF ZINC OXIDE-GRAPHENE NANOCOMPOSITES

HARISH KUMAR*, MANISHA KUMARI

Department of Chemistry, Material Science and Nano Materials Laboratory, Ch. Devi Lal University, Sirsa - 125 055, Haryana, India.
Email: harimoudgil1@gmail.com

Received: 01 May 2017, Revised and Accepted: 27 May 2017

ABSTRACT

Objectives: A novel facile synthesis of zinc oxide (ZnO) and zinc-graphene oxide nanocomposites (ZnGONC) was achieved by modified sol-gel technique for their pharmaceutical and therapeutic use.

Materials and Methods: Spherical, crystalline, defect-free Zinc oxide nanoparticles (ZnO NPs) with diameter 70-90 nm were synthesized by modified sol-gel technique. Reduced graphene oxide was synthesized by modified Hummers method. ZnGONC were synthesized by *in situ* method. The crystalline nature, size, shape, and dimensions of the NPs, graphene oxide, and nanocomposites were studied by X-ray diffraction method. Transmission electron microscopy analysis was carried out to examine the morphology of NPs and nanocomposites.

Results: Fourier transform infrared spectroscopy analysis confirms that the ZnO NPs are surrounded by oxygen and silicon atoms. Antibacterial activity of ZnO NPs and ZnGONC was investigated against Gram-positive and Gram-negative bacteria. Zone of inhibition shown by ZnO NPs and ZnGONC was found to be higher than six investigated standard antibiotics.

Conclusion: Synthesized ZnO NPs and nanocomposites can be used as antibacterial agents. This eco-friendly method of synthesis of ZnO NPs and ZnGONC could be a viable solution for industrial applications in the future and therapeutic needs.

Keywords: Sol-gel, Zinc oxide nanoparticles, Optical properties, Nanocomposites, Antibacterial property.

© 2017 The Authors. Published by Innovare Academic Sciences Pvt Ltd. This is an open access article under the CC BY license (<http://creativecommons.org/licenses/by/4.0/>) DOI: <http://dx.doi.org/10.22159/ajpcr.2017.v10i9.19459>

INTRODUCTION

Nanotechnology has emerged as a valuable modus in the pharmaceutical industry as an alternative antimicrobial approach because of arrival of antibiotic-resistant strains of microorganisms [1]. Nanosized particles, either simple or composite by nature, exhibit unique physical and chemical properties and show a potential of being used in various biomedical application [2-9]. There is a need to develop uniform nanosize drug particles having precise shape, size, and physical and chemical properties in the production of new pharmaceutical products. The biocidal efficiency of nanoparticles (NPs) may be due to combination of small size and high surface to volume ratio which facilitates intimate interactions with microbial membranes [10,11].

Metal oxides with nanostructure have attracted considerable interest in many areas of technology [12]. Among metal oxide NPs, zinc oxide (ZnO) has received much attention in the recent past. ZnO nanostructures are the forefront of research due to their unique properties and wide applications such as ultraviolet blocking properties [13]. The advantage of using ZnO NPs is that they strongly inhibit the action of pathogenic microbes when used in small concentration [14].

Graphene oxide (GO) which is actually a compact honeycomb structure of sp^2 hybridized carbon atoms has drawn a huge attention because of its outstanding electronic, thermal, and mechanical properties, which can be applied in nanomedicine field [15-20]. GO can be used to stabilize growing metal NPs and inhibits their aggregation because of its unique properties such as large surface area, low cytotoxicity, and good water stability. On these basis, GO and its composites have a wide range of possible applications on transistors, transparent conductors, polymer reinforcement, bioengineering, and biomaterials areas [21-23].

A lot of research has been carried out on antibacterial properties of Ag NPs and their nanocomposites. In continuation to our earlier study [24-30], in the present study, we have focused on the synthesis of zinc (Zn) NPs by facile, and cost effective sol-gel method and nanocomposite of Zn were prepared with reduced graphene oxide (RGO). Antibacterial properties of the synthesized NPs and nanocomposites were investigated against Gram-positive and Gram-negative bacteria. The aim of this study is to synthesize a nanocomposite material with better or comparable antibacterial performance.

MATERIALS AND METHODS

Materials

All chemicals used were of analytical reagent grade and used without further purification. Chemicals used were graphite powder (<20 μ), $ZnCl_2$, $NaNO_3$, H_2O_2 , H_2SO_4 , $KMnO_4$, HCl, NaOH, $NaBH_4$, citric acid, and ethylene glycol. All were available in our research lab. The strains employed in this work were the Gram-negative bacterium (*Escherichia coli*) and Gram-positive bacterium (*Staphylococcus epidermidis*). In addition, nutrient broth and agar-agar were used to prepare agar plates.

Preparation of RGO

GO was synthesized from graphite powder by a modified Hummers method [31]. Graphite powder, $NaNO_3$, and H_2SO_4 were mixed together at 0.0°C. Then, $KMnO_4$ was added slowly into the reaction mixture with constant stirring. The mixture was heated to 35.0°C and stirred for 12.0 hrs, and then, 500.0 mL of water was slowly added under vigorous stirring. Then, 30.0% H_2O_2 solution was added to reduce the residual MnO_2 . The mixture was then washed by acidified water (3.0%) and then with double distilled water three times followed by filtration and drying. RGO sheets were then obtained.

Preparation of ZnO NPs

ZnCl₂ solution and citric acid solution were prepared separately in double-distilled water and were mixed together with continuous stirring for 15.0 minutes. Ethylene glycol was then added into the solution and continuously stirred for 3 hrs. The resultant precipitates thus obtained were washed with double-distilled water and then dried at 100.0°C in oven for 2.0 hrs. Finally, these were put into the muffle furnace at 600.0°C for 2.0 hrs. ZnO NPs were thus obtained.

Preparation of ZnO/GO nanocomposites

ZnCl₂ and GO were mixed together in double-distilled water to have a metal oxide loading of 10 wt%. The solution pH was adjusted to 10.0 using NaOH solution and stirred continuously for 4.0 hrs. Then, 50 ml of 0.1 M NaBH₄ was added and stirred continuously for 3.0 hrs. The resulting material was then filtered and washed several times with double-distilled water and dried in oven at 80.0°C. It was then calcined at 400.0°C for 3.0 hrs.

Table 1: ZOI (mm) shown by different standard antibiotics with *Staphylococcus epidermidis* and *Escherichia coli*

Bacterium	Standard antibiotics					
	TE 25	C 25	P ₁	AMP 10	S 10	S3 300
<i>Staphylococcus epidermidis</i>	19	17	15	NS	23	NS
<i>Escherichia coli</i>	11	9	NS	NS	13	NS

ZOI: Zone of inhibition

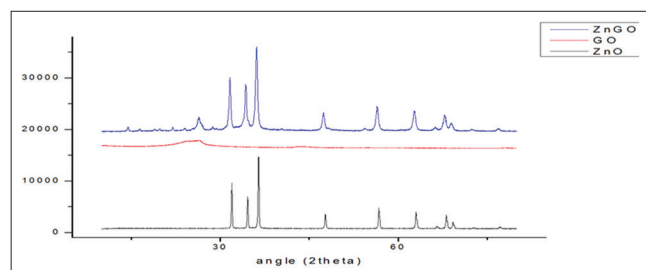


Fig. 1: X-ray diffractometer of zinc oxide nanoparticles, reduced graphene oxide, and zinc-graphene oxide nanocomposite

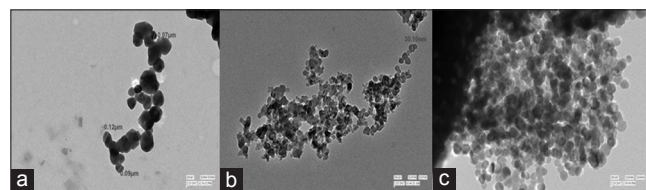


Fig. 2: Transmission electron microscopy images of (a) zinc oxide nanoparticles, (b) reduced graphene oxide, (c) zinc-graphene oxide nanocomposite

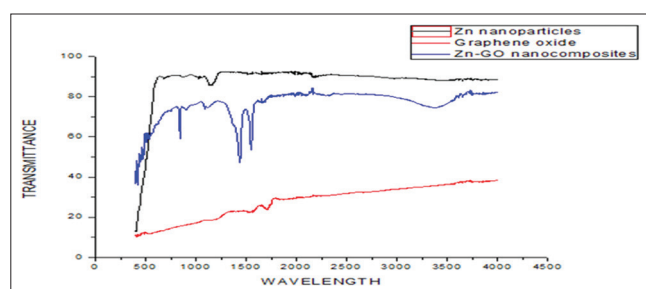


Fig. 3: Fourier transform infrared spectra of zinc oxide nanoparticles, reduced graphene oxide and zinc oxide graphene oxide nano-composites

RESULTS AND DISCUSSION

Characterizations

The X-ray diffraction pattern of the ZnO NPs and ZnO-GO nanocomposites samples were obtained (Fig. 1) using an X-ray diffractometer (XRD) (Panalyticals X.Pert Pro, P.U. Chandigarh). The XRD pattern of RGO indicates a broad diffraction peak at $2\theta=24^\circ$. The broadening and shift of the characteristic diffraction peak of graphite from 26.58° to 24° in RGO which was due to the short-range order in stacked stacks. All XRD diffraction peaks of ZnO powders are shown in good agreement with hexagonal structure of ZnO reported in JCPDS File Card No. 05-0664. Peaks of ZnO at 31.7° , 34.4° , 36.2° , 47.4° , 56.6° , 62.9° , 65.5° , 68.0° , and 69.1° that are corresponding to (100), (002), (101), (102), (110), (103), (200), (112), and (201) lattice planes, respectively, indicating the formation of the wurtzite structure of ZnO NPs. No peaks of impurity are observed, indicating that the high purity ZnO was obtained. The XRD spectra of nanocomposites have peaks corresponding to both RGO and ZnO NPs.

The size, morphology, and distribution of ZnO NPs in ZnO-GO nanocomposites were examined using a transmission electron microscopy (TEM) (TECNAI 200 Kv TEM [Fei, Electron Optics], AIIMS, Delhi). Fig. 2 shows TEM images of ZnO NPs, (a) RGO, and (b) ZnO-GO nanocomposite, and (c) the inset of Fig. 2a shows that the ZnO NPs have a spherical shape. The TEM image reveals that the ZnO NPs are dispersed on the GO (Fig. 2c). In addition, the TEM image shows an average particle size of approximately 90 nm for the NPs. From the TEM images, the GO surface looks smooth and integrated (Fig. 2b). In the case of ZnO-GO nanocomposite (Fig. 2c), a large number of ZnO nanocomposites with average diameters 21.7 ± 2.3 nm were observed

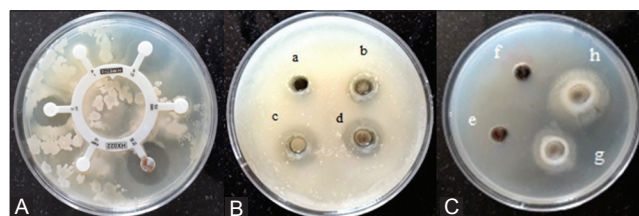


Fig. 4: (A) Zone of inhibition (ZOI) produced by different standard antibiotics with *Staphylococcus epidermidis* (B) and (C) different concentration of zinc oxide nanoparticles (ZnO-NPs) and ZnO-graphene oxide (ZnO-GO) nanocomposites. ZOI produced with *S. epidermidis*, (a) ZnSO₄, (b) 100 ppm concentration of ZnO-NPs, (c) 500 ppm concentration of ZnO-NPs, (d) 1000 ppm concentration of ZnO-NPs, (e) ZnSO₄ and grapheme, (f) 100 ppm concentration of ZnO-GO nanocomposites, (g) 500 ppm concentration of ZnO-GO nanocomposites, (h) 1000 ppm concentration of ZnO-GO nanocomposites

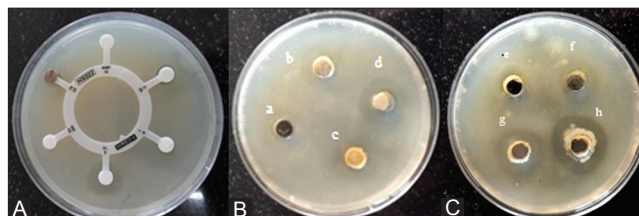


Fig. 5: Zone of inhibition (ZOI) produced by different standard antibiotics with *Escherichia coli* (A) and different concentration of zinc oxide nanoparticles (ZnO-NPs) (B) and ZnO-graphene oxide (GO) nanocomposites (C) with bacteria. ZOI produced with *E. coli*, (a) ZnSO₄, (b) 100 ppm concentration of ZnO-NPs, (c) 500 ppm concentration of ZnO-NPs, (d) 1000 ppm concentration of ZnO-NPs, (e) ZnSO₄ and grapheme, (f) 100 ppm concentration of ZnO-GO nanocomposites, (g) 500 ppm concentration of ZnO-GO nanocomposites, (h) 1000 ppm concentration of ZnO-GO nanocomposites

Table 2: Antibacterial effect of ZnO NPs and ZnO-GO nanocomposites against Gram-positive (*Staphylococcus epidermidis*) and Gram-negative (*Escherichia coli*) bacteria is indicated by measuring the diameter of ZOI (mm)

Bacterial test organism	Sample concentration in µg/ml				Sample concentration in µg/ml			
	ZnSO ₄		ZnO NPs		ZnSO ₄ +graphene		ZnO-GO nanocomposites	
	1000	100	500	1000	1000	100	500	1000
<i>Staphylococcus epidermidis</i>	0	12	17	19	0	13	24	28
<i>Escherichia coli</i>	0	16	19	21	10	17	20	23

ZnO NPs: Zinc oxide nanoparticles, ZnO-GO: Zinc oxide-graphene oxide, ZOI: Zone of inhibition

uniformly on the surface of the GO. The high-magnification TEM image (Fig. 2c) further reveals that ZnO-GO nanocomposites are almost spherical in shape.

The chemical functional groups of ZnO NPs and ZnO-GO nanocomposites were characterized using attenuated total reflectance Fourier transform infrared (FTIR) spectrometer (Perkin Elmer - Spectrum RX-IFTIR, P.U. Chandigarh). Fig. 3 shows FTIR spectra of ZnO NPs, RGO, and Zn-GO nanocomposites. In the FTIR spectrum for RGO, the peaks at 1731, 1625, and 1183 cm⁻¹ are assigned to the C=O stretching, C=C stretching, and C-O stretching, respectively. The broad peak at 3250 cm⁻¹ in the FTIR spectrum of the ZnO-NPs/GO nanocomposite might be attributed to the O-H stretching vibration of absorbed water molecules. The following functional groups were identified; O-H stretching vibrations (3240-3300 cm⁻¹), C=O stretching vibration (1720-1740 cm⁻¹), C=C from un-oxidized sp² C-C bonds (1590-1620 cm⁻¹), and C-O vibrations (1250 cm⁻¹) in the FTIR spectrum of ZnO-GO nanocomposites which confirms the formation of nanocomposites.

Antibacterial study

The different researchers have reported antibacterial property of different metal NPs [32-35]. We have tested antibacterial activity of the ZnO NPs and ZnO-GO nanocomposites on Gram-positive (*S. epidermidis*) and Gram-negative (*E. coli*) bacteria using agar well diffusion method. Table 1 shows zone of inhibition (ZOI) (mm) shown by different standard antibiotics with *S. epidermidis* and *E. coli*. Table 2 shows antibacterial effect of ZnO NPs and ZnO-GO nanocomposites against Gram-positive (*S. epidermidis*) and Gram-negative (*E. coli*) bacteria are indicated by measuring the diameter of ZOI (mm). Fig. 4 shows that ZOI produced by different standard antibiotics with *S. epidermidis* (a) and different concentration of ZnO-NPs and ZnO-GO nanocomposites (b) and (c). Fig. 5 shows that ZOI shown by different standard antibiotics with *E. coli* (d) and different concentration of ZnO-NPs (e) and ZnO-GO nanocomposites (f) with bacteria.

Agar plates were prepared using nutrient broth and agar-agar. The wells of 8.0 mm diameter were punched with the help of steel borer into the agar having the test microorganism (at concentration about 5×10⁵ CFU/ml). The wells were filled with 100.0 µl of ZnO NPs and ZnO-GO nanocomposites of different concentration. A range of standard antibiotics (Hexa disc) was also used as the control. After 24.0 hrs incubation at 37.0°C, the diameters of the inhibition zones were measured against the test microorganisms and optical images were documented by a high definition optical camera.

The highest ZOI shown by standard antibiotics is 23.0 and 13.0 for *S. epidermidis* and *E. coli*, respectively. The highest ZOI shown by ZnO NP and ZnO-GO nanocomposites is 28.0 and 23.0 for *S. epidermidis* and *E. coli*, respectively. Hence, both ZnO and ZnO-GO nanocomposites show better antibacterial properties than six standard investigated antibiotics.

CONCLUSION

ZnO NPs, RGO, and ZnO-GO nanocomposites have been prepared through facile and easy sol-gel methods. ZnO NPs samples exhibit good antibacterial activities against Gram-negative bacterial strain *E. coli* and Gram-positive strain *S. epidermidis*, but ZnO-GO nanocomposites

exhibit better antibacterial activity. The increase of concentration of both ZnO NPs and ZnO-GO nanocomposites results in increase in antibacterial activity. Antibacterial property of both, i.e., ZnO NPs and ZnO-GO nanocomposites was compared with six standard antibiotics. The highest ZOI shown by standard antibiotics is 23.0 and 13.0 for *S. epidermidis* and *E. coli*, respectively. Highest ZOI shown by ZnO NP and ZnO-GO nanocomposites is 28.0 and 23.0 for *S. epidermidis* and *E. coli*, respectively. Hence, both ZnO and ZnO-GO nanocomposites show better antibacterial properties than six standard investigated antibiotics.

REFERENCES

- Desselberger U. Emerging and re-emerging infectious diseases. *J Infect* 2000;40(1):3-15.
- Chan WC, Nie S. Quantum dot bioconjugates for ultrasensitive nonisotopic detection. *Science* 1998;281(5385):2016-8.
- Alivisatos AP. Semiconductor clusters, nanocrystal, and quantum dots. *Science* 1996;271(5251):933.
- Chan WC, Maxwell DJ, Gao X, Bailey RE, Han M, Nie S. Luminescent quantum dots for multiplexed biological detection and imaging. *Curr Opin Biotechnol* 2002;13(1):40.
- Wu X, Liu H, Liu J, Haley KN, Treadway JA, Larson JP, *et al.* Quantum dots for live cells. *Nat Biotechnol* 2003;21:41.
- Brigger I, Dubernet C, Couvreur P. Nanoparticles in cancer therapy and diagnosis. *Adv Drug Deliv Rev* 2002;54(5):631-51.
- Forestier F, Gerrier P, Chaumard C, Quero AM, Couvreur P, Labarre C. Effect of nanoparticle-bound ampicillin on the survival of *Listeria monocytogenes* in mouse peritoneal macrophages. *Antimicrob Chemother* 1992;30(2):173-9.
- Sondi I, Siiman O, Koester S, Matijevic E. Preparation of aminodextran-CdS nanoparticle complexes and biologically active antibody-aminodextran-CdS nanoparticle conjugates. *Langmuir* 2000;16(7):3107-18.
- Siiman O, Matijevic E, Sondi I. Semiconductor nanoparticles for analysis of blood cell populations and methods of making same. U.S. Patent 6235540 B1.
- Allaker RP. The use of nanoparticles to control oral biofilm formation. *J Dent Res* 2010;89(11):1175-86.
- Morones JR, Elechiguerra JL, Camacho A, Holt K, Kouri JB, Ramirez JT, *et al.* The bactericidal effect of silver nanoparticles. *Nanotechnology* 2005;16:2346-53.
- Sangeetha G, Rajeshwari S, Venkatesh R. Green synthesis of zinc oxide nanoparticles by aloe barbadensis miller leaf extract: Structure and optical properties. *Mat Res Bull* 2011;46(12):2560-6.
- Rouhi J, Mahmud S, Naderi N, Ooi CH, Mahmood MR. Physical properties of fish gelatin-based bio-nanocomposite films incorporated with ZnO nanorods. *Nanoscale Res Lett* 2013;8:364.
- Appelrot K, Wiberg E, Holleman AF. *Inorganic Chemistry*. Vol. 22. Amsterdam: Elsevier; 2009. p. 24-34.
- Novoselov KS, Geim AK, Morozov SV, Jiang D, Katsnelson MI, Grigorieva IV, *et al.* Two-dimensional gas of massless dirac fermions in graphene. *Nature* 2005;438(706):197-200.
- Li X, Wang X, Zhang L, Lee S, Dai H. Chemically derived, ultra smooth graphene nanoribbon semiconductors. *Science* 2008;319(5867):1229-32.
- Stankovich S, Dikin DA, Dommett GH, Kohlhaas KM, Zimney EJ, Stach EA, *et al.* Graphene-based composite materials. *Nature* 2006;442(7100):282-6.
- Xiao W, Zhang YH, Liu BT. Raspberry-like SiO₂@reduced graphene oxide@AgNP composite microspheres with high aqueous dispersity and excellent catalytic activity. *ACS Appl Mater Interfaces* 2005;7(11):6041-6.
- Xiao W, Zhang Y, Tian L, Liu H, Liu B, Pu Y. Facile synthesis of

- reduced graphene oxide/titania composite hollow microspheres based on sonication-assisted interfacial self-assembly of tiny graphene oxide sheets and the photocatalytic property. *J Alloys Compounds* 2016;665(25):21-30.
20. Schedin F, Geim AK, Morozov SV. Detection of individual gas molecules adsorbed on graphene. *Nat Mater* 2007;6(9):652-5.
 21. Liao KH, Lin YS, Macosko CW, Haynes CL. Cytotoxicity of graphene oxide and graphene in human erythrocytes and skin fibroblasts. *ACS Appl Mater Interfaces* 2011;3(7):2607-15.
 22. Ruiz ON, Fernando KA, Wang B, Brown NA, Luo PG, McNamara ND, et al. Graphene oxide: A nonspecific enhancer of cellular growth. *ACS Nano* 2011;5(10):8100-7.
 23. Kavitha T, Gopalan AI, Lee KP, Park SY. Glucose sensing, photocatalytic and antibacterial properties of graphene-ZnO nanoparticle hybrids. *Carbon* 2012;50(8):2994-3000.
 24. Sangwan P, Kumar H. Synthesis, characterization, and antibacterial activities of chromium oxide nanoparticles against *Klebsiella pneumoniae*. *Asian J Pharm Clin Res* 2017;10(2):1-4.
 25. Sangwan P, Kumar H, Purewal SS. Antibacterial activity of chemically synthesized chromium oxide nanoparticles against enterococcus *Faecalis*. *Int J Adv Technol Eng Sci* 2016;4(8):550-6.
 26. Kumar H, Bhawana R. Synthesis of metal nanoparticles & their use in electrochemical biosensors for the detection of microbes. *Int J Ad Res Sci Eng* 2016;5(8):751-61.
 27. Rani R, Kumar H, Salar RK, Purewal SS. Antibacterial activity of copper oxide nanoparticles against gram-negative bacterial strain synthesized by reverse micelle route. *Int J Pharm Res Dev* 2014;6(1):72-8.
 28. Kumar H, Manisha P, Sangwan P. Synthesis & characterization of MnO₂ nanoparticles using co-precipitation technique. *Int J Chem Chem Eng* 2013;3(3):155-60.
 29. Kumar H, Rani R. Structural characterization of silver nanoparticles synthesized by microemulsion route. *Int J Eng Innov Technol* 2013;3(3):344-8.
 30. Kumar H, Rani R. Structural and optical characterization of ZnO nanoparticles synthesized by microemulsion route. *Int Lett Chem Phys Astron* 2013;14:26-36.
 31. Hummers WS, Offeman RE. Preparation of graphitic oxide. *J Am Chem Soc* 1958;80(6):1339-9.
 32. Bhatta P, Deepthi S, Kumarb CH, Jha A. Facile synthesis, spectral studies, DFT calculations and biological activities of novel Ni (ii), Cu (ii), and Pd (ii) complexes of thiazole analogs. *Int J Pharm Pharm Sci* 2017;9(7):185-95.
 33. Rohit M, Showkat RM, Saima A. Polymeric nanoparticles for improved bioavailability of cilnidipine. *Int J Pharm Pharm Sci* 2017;9(4):129-39.
 34. Murugesan S, Bhuvaneshwari S, Sivamurugan V. Green synthesis, characterization of silver nanoparticles of a marine red alga *Spyridia fusiformis* and their antibacterial activity. *Int J Pharm Pharm Sci* 2017;9(5):192-7.
 35. Safdar MH, Hasan H, Anees M, Hussain Z. Folic acid-conjugated doxorubicin-loaded photosensitizing manganese ferrite nanoparticles: Synthesis, characterization and anticancer activity against human cervical carcinoma cell line (HELA). *Int J Pharm Pharm Sci* 2017;9(5):60-7.